High Resolution Topography of the Central San Andreas Fault at Dry Lake Valley, California, USA

Michael P. Bunds[1] (michael.bunds@uvu.edu), Chelsea Scott[2], Nathan A. Toké[1], Jeremy Saldivar[1], Logan Woolstenhulme[1], Joseph Phillips[1], Marissa Keck[1], Serena Smith[1], and McKenzie Ranney[1]

[1] Department of Earth Science, Utah Valley University, 800 West University Parkway, Orem, UT 84058
[2] School of Earth and Space Exploration, Arizona State University, Tempe, AZ 85287

DOI:

Introduction

This document accompanies high-resolution topography and an orthomosaic of a portion of the central San Andreas Fault, California, USA. The data set was generated from optical photographs taken with a small uncrewed aerial system (sUAS) and differential global navigation satellite system (dGNSS) measurements using structure-from-motion processing (SfM) and covers ~ 3 km of strike length of the fault (Figure 1). We acquired this data set to measure tectonic deformation near the fault (Scott et al., in review). An overview of the data set and methods used to create it is provided here, and includes a discussion of the motivation and purpose of the data, a description of the data products, overviews of collection of raw data in the field and data processing, and a summary of the uncertainty in the topographic model. The data set is available free-to-public on OpenTopography.org, and more information may be obtained from Michael Bunds at Utah Valley University (michael.bunds@uvu.edu).

Background

Much of the relative motion between the North America and Pacific Plates is accommodated along the San Andreas fault (SAF) transform plate boundary in California, USA. The central section of the SAF is known to creep aseismically at up to ~ 3 cm / yr (see Scott et al., in review, and references therein). The primary motivation for generation of this high resolution topography was to image displacement and displacement gradients (i.e., strain) along and across the fault by differencing the data against airborne LiDAR collected in 2007 as part of the EarthScope project (EarthScope, 2008). The sUAS data was collected at the Dry Lake Valley (DLV) paleoseimic study site, because information from studies of surface fracturing and paleoseismology is available from there (Toke and Arrowsmith, 2015; Scott et al., in review).

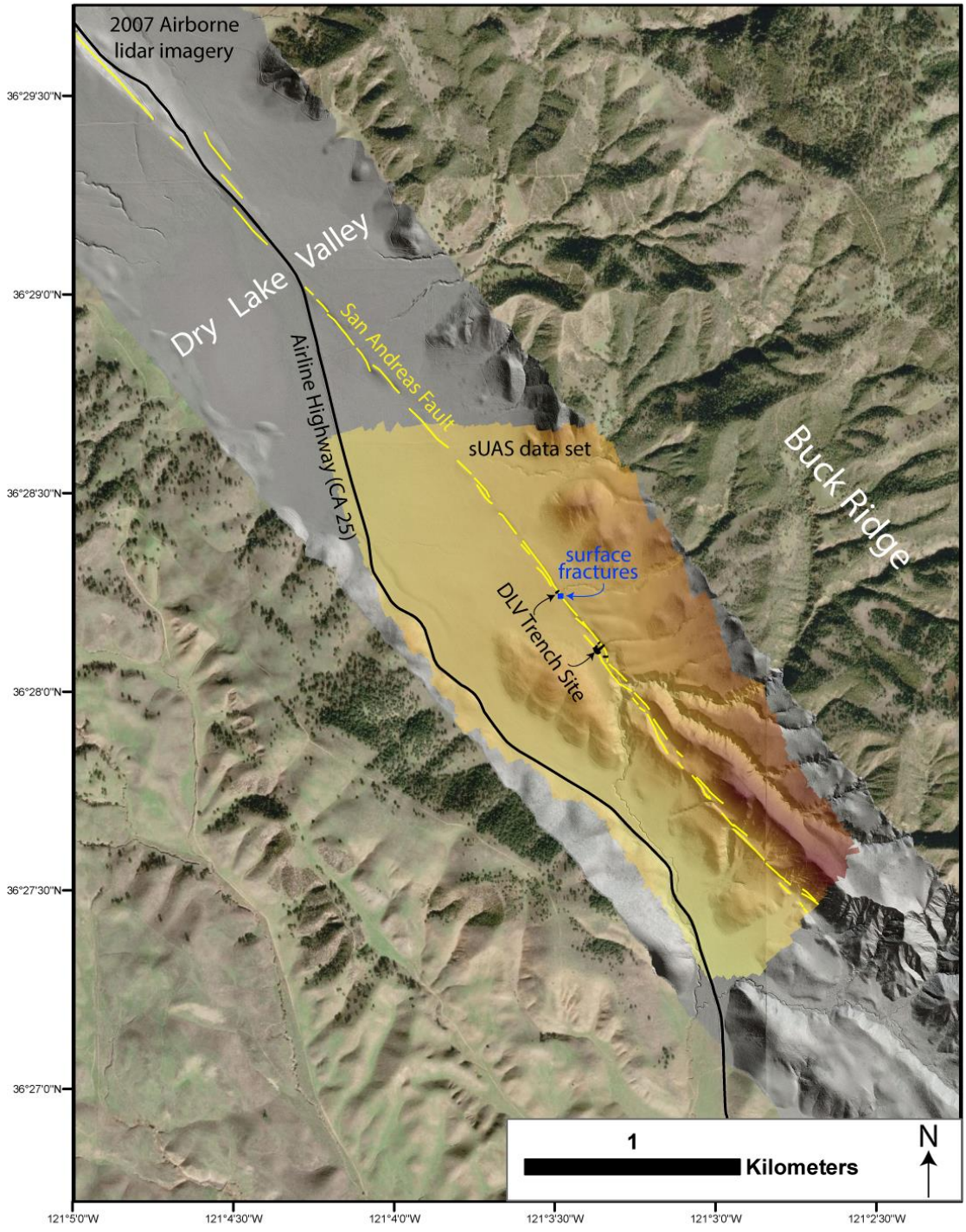

Figure 1. Location map showing area covered by the topographic data set. From Scott et al., in review.

Data Description (Table 1)

1. Point cloud model of the DLV study site. The point cloud contains 1.192 x 10^9 points each with a color attribute. A subset of the points are classified as ground (see processing notes below for a description of the classification procedure). The point cloud covers approximately 2.74 km^2, for an average point density of 435 points/m^2. The point cloud is in the reference frame IGS00, UTM zone 10 (EPSG 32610), epoch 2007.2274, and ellipsoidal heights (units of meters), as is the entire data set. The reference frame was chosen to match EarthScope LiDAR of the area collected in 2007 (EarthScope, 2008); see processing notes below for more information on how the data were georeferenced.
2. Digital surface model (DSM) that has a 0.06-m pixel spacing and covers the same area as the point cloud. The DSM was rasterized from the point cloud in Agisoft Metashape (v1.6.1), using a 'binning' algorithm, wherein each DSM pixel value (elevation) is calculated as an average of the elevation of points located within the pixel area. All points in the point cloud, regardless of their classification, were used. The DSM reference frame is IGS00, UTM zone 10 (EPSG 32610), epoch 2007.2274, and ellipsoidal heights (units of meters).
3. Orthomosaic, with a 0.03-m pixel size. The orthomosaic was constructed from the aerial photographs in Agisoft Metashape using the DSM to orthorectify the imagery and by blending the individual photos together. The reference frame is IGS00, UTM zone 10 (EPSG 32610), epoch 2007.2274.
4. Table of camera locations. The topographic model was constructed and georeferenced from low altitude aerial photographs collected with a Sensefly eBee Plus, which collects dGNSS data and photograph time stamps that provide a precise camera position for each photograph. A table of the locations from which the photographs were taken is provided. The reference frame is IGS00, UTM zone 10 (EPSG 32610), epoch 2007.2274, and ellipsoidal heights (units of meters). See georeferencing section below for more information.
5. Table of ground control point (GCP) locations. GCPs consisted of markers placed on the ground and visible in aerial photographs. The positions of the GCPs were surveyed with differential GNSS and they were used in conjunction with photograph locations to georeference the topographic model. A table of the locations of the GCPs is provided as a comma-delimited digital file. The reference frame is IGS00, UTM zone 10 (EPSG 32610), epoch 2007.2274, and ellipsoidal heights (units of meters). See georeferencing section below for more information.

Data Collection Overview

Field work to acquire the high-resolution topography was conducted on October 27 and 28, 2017. A Sensefly eBee Plus equipped with a SODA camera and onboard dual frequency dGNSS was used to collect 3533 aerial photographs of the study site.

Flight plans for photograph acquisition were generated in Sensefly eMotion software. The plans included the area to be imaged, photograph ground sample distance, and photograph overlap. Ground sample distance averages 2.77 cm/pixel, and average camera altitude above ground level was 120 to 130 m. Flight altitude exceeds 100 m above ground on average in order to maintain ~100 m altitude over hills and vegetation. Average photograph overlap estimated from the number of photographs in which each GCP appears is 26x (i.e., each GCP appears in 26 photographs on average). Overlap as

calculated by Agisoft Metashape is > 9x over nearly the entire study area, with the primary exceptions being some areas along the edge of the model. A total of six flights of the eBee were flown.

Structure-from-Motion Processing

Processing of the photographs to produce the point cloud, DSM and orthomosaic was done with Agisoft Metashape using the following workflow. Camera models and a sparse cloud (tie points) were generated using the 'highest' setting. The models and sparse cloud were then georeferenced and optimized using measured camera positions for each photograph and GCP positions (see georeferencing section below). The position of every GCP was manually marked by hand in every photograph in which it clearly appears prior to optimization of the sparse point cloud and camera model. Agisoft fit a modified Brown-Conrady camera distortion model (an apriori camera distortion model was not used). Sparse cloud points with reconstruction uncertainty greater than 10 or reprojection error greater than 0.3 were then removed incrementally in conjunction with re-optimization of the sparse cloud. The dense point cloud was generated using the 'high' setting (i.e., photos were downsampled x2). Model data parameters are summarized in Table 1.

Table 1. Summary of Topographic Model Parameters

Parameter	DLV topographic model
Total points	1.192×10^9
Coverage area	2.74 km^2
Point density	435 points/m^2
Number photographs	3,533
Average GSD	0.028 m
Number GCPs	30
Number checkpoints	18
Checkpoint RMSerror	0.038 m
DSM resolution	0.060 m
Orthomosaic resolution	0.030 m
Horizontal reference frame – point clouds, DSMs and orthomosaics	IGS00 UTM Zone 10 (EPSG 32610) epoch 2007.2274
Vertical reference frame	IGS00 Ellipsoid
Field data collection date	October, 2017

The edges of the point cloud were trimmed to remove areas with poor photograph overlap and less reliable SfM construction. However, because the remaining model extends beyond the outermost camera locations, it should be expected that the accuracy of the topographic model on the edges is reduced due to less photograph overlap and limited camera view directions (and larger reconstruction uncertainty).

A subset of points in the point cloud were classified as ground using LasTools. The 'wilderness ground classification' in lasground_new was applied to remove features with a 3 m length or smaller (Isenberg, 2019), as shown in Figure 2. Scott et al. (in review) found that the wilderness setting produced lower error in the 3D displacements produced by differencing this sUAV dataset with the EarthScope dataset than other ground classification options. The other options remove larger scale features and typically classify more points as ground. The ground point classification procedure removes objects identified as vegetation based on shape and produces different results than classification procedures based on return number that can be applied to LiDAR point clouds.

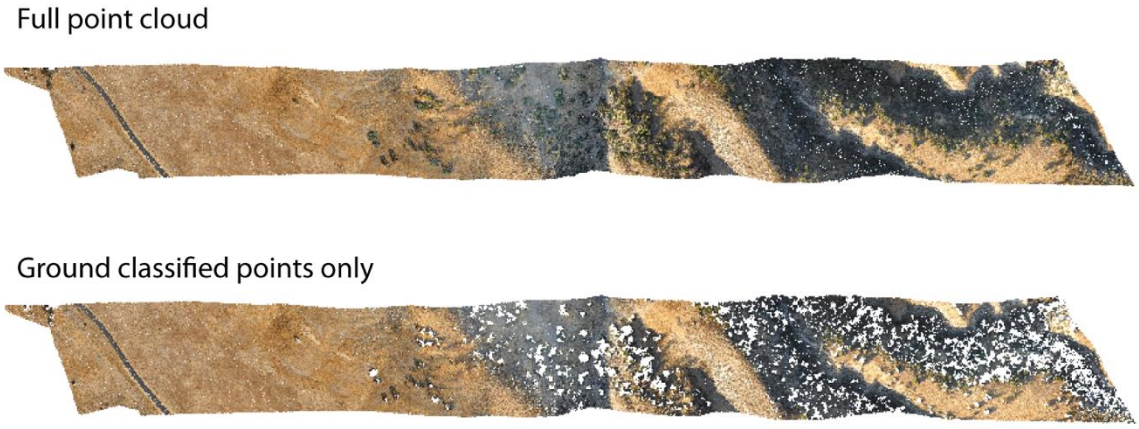

Figure 2: Wilderness ground classification. **Top:** Full point cloud. **Bottom:** Ground classified points only.

The DSM was made in Agisoft Metashape using all points in the point cloud, regardless of their classification. The value for each DSM pixel is a direct average of the elevation values of points within the pixel square area. The DSM was made directly from the point cloud without construction of a TIN mesh.

The orthomosaic was made in Agisoft using the default blending mode. The DSM was used to orthorectify the images.

SfM computer processing was done on a suite of workstations in the Geospatial Laboratory at Utah Valley University, and point classification was performed at Arizona State University.

Georeferencing and Accuracy

All data (point cloud, DSM, orthomosaic, and accompanying GCP and camera locations) were effectively placed in the reference frame IGS00, UTM zone 10 (EPSG 32610), epoch 2007.2274, and ellipsoidal heights (units of meters). The reference frame was chosen to match the 2007 EarthScope LiDAR that also covers the study area (EarthScope, 2008). Camera positions and GCPs were used to georeference the data. Camera and GCP locations were measured using dGNSS and a local reference station, and transformed into IGS00 epoch 2007.2274.

A local reference station was established at the study area. The local reference station consisted of a Septentrio PolaRx5 receiver and Trimble Zephyr Geodetic 2 antenna, placed over a survey marker made

by drilling a small hole in a concrete slab. The reference station was operated for approximately 13 hours, and its position was determined using the National Geodetic Survey's Online Positioning User Service (NGS OPUS) and precise ephemeri. Reference station uncertainty is estimated to be approximately +/- 0.003 m and 0.006 m in the horizontal and vertical directions, respectively.

The Sensefly eBee Plus incorporated a multiple frequency dGNSS system that recorded positions at 1 Hz and a time stamp for each photograph. The camera positions for each photograph were post-processed (i.e., PPK) using Sensefly/Septentrio's software and the local base data and position. The software calculates the position of the camera for each photograph by interpolating the dGNSS 1 Hz results and adjusting for the camera offset (i.e., position of the camera relative to the GNSS antenna phase center). The camera positions were uploaded into Agisoft and a table of camera positions is included with the metadata. Camera position uncertainty is estimated to range from +/- 0.005 m (horizontal) and 0.010 m (vertical) to +/- 0.050 m (horizontal) and 0.100 m (vertical) for the ~3500 photographs for which fixed PPK solutions were determined, with ~80% having uncertainties less than +/- 0.020 m (horizontal) and 0.040 m (vertical).

Thirty GCPs were also used for georeferencing. GCPs consisted of markers placed on the ground, the positions of which were measured using dGNSS that was collected in kinetic mode and post-processed against the local reference station using Trimble Business Center. 30 GCPs were used and a table of GCP positions is included as metadata. During SfM processing, the position of every GCP was manually marked by hand in every photograph in which it clearly appears using Agisoft Metashape prior to optimization of the sparse point clouds and camera models. GCP location measurement uncertainty is estimated to vary from +/- 0.01 m (horizontal) and +/- 0.015 m (vertical) up to approximately +/- 0.02 m (horizontal) and +/- 0.04 m (vertical). Additional uncertainty of ~1 to 4 cm in the vertical direction is possible due to movement of the GCP markers due to wind and during measurement.

The topographic model was adjusted downward 10.2 cm to remove a vertical bias relative to GCPs and checkpoints. It is likely that the vertical bias is the result of systematic error in the camera lens model. We have found similar biases in all other models that we have georeferenced with camera positions determined directly from dGNSS onboard the sUAS.

The data were placed into the IGS00 epoch 2007.2274 reference frame to match the EarthScope LiDAR of the area (EarthScope, 2008). The local reference station position was originally determined in IGS08 epoch 2017.8229 using the NGS OPUS system. The reference station position was then transformed into IGS00 epoch 2007.2274 using the NGS Horizontal Time Dependent Positioning calculator, which accounts for both reference frame migration and plate motion. Processing in Agisoft Metashape was done in the WGS84 ellipsoid.

Vertical accuracy of the final DSM was assessed using checkpoints. Checkpoints are dGNSS measurements taken away from GCPs on bare, relatively flat ground. Eighteen checkpoint measurements were made across the study area. The elevation predicted for each checkpoint was extracted from the DSM using ArcMAP, and a residual was calculated by taking the difference between the DSM elevation and the directly measured elevation for each checkpoint. Root-mean-square error (RMSe; 1-sigma error) calculated from the residuals for all checkpoints 3.8 cm. RMSe in the horizontal is estimated to be ~2.1 cm based on misfit to GCP targets used as checkpoints for a topographic model made using camera positions only. Camera positions, GCPs and checkpoints were measured using the same reference station as the GCPs, so some additional absolute error on the order of +/- 0.003 m

(horizontal) and 0.006 m (vertical) should be expected to be present in the data set due to error in the measured position of the reference station. Note that misfit of the point clouds to camera positions and GCPs (as measured by Agisoft) is much less than checkpoint error, and reflects the fact that GCP misfit as calculated in Agisoft is not a reliable measure of model accuracy across the survey area.

Although we have endeavored to minimize and quantify error in the data set, no guarantee of accuracy is given nor implied. In addition, DSM and point cloud error should be expected to vary across the data set. dGNSS processing was conducted at the Geospatial Laboratory at Utah Valley University.

References Cited

EarthScope, 2008, EarthScope Northern California LiDAR Project. NSF OpenTopography 667 Facility. https://doi.org/10.5069/G9057CV2

Isenburg, M., 2019, *LAStools - Efficient tools for lidar processing*. Retrieved from www.lastools.org.

Scott, C., Bunds, M.P., Shirzaei, M., Toke, N., in review, Creep along the Central San Andreas Fault imaged from surface fractures, topographic differencing, and InSAR imagery, Journal of Geophysical Research.

Toké, N. A., & Arrowsmith, J. R., 2015, Examining the Cause of Prehistoric Ground Deformation at the Dry Lake Valley Site along the Creeping Section of the San Andreas Fault, San Benito, California, Southern California Earthquake Center Technical Report No. 13147: https://www.scec.org/proposal/report/13147

Acknowledgements

This project was supported by awards to Bunds from Utah Valley University's Office of Engaged Learning and College of Science Scholarly Activities Committee; and by the National Science Foundation Postdoctoral Fellowship 1625221 to Scott. We also thank NVIDIA for a GPU Grant and acknowledge the support of Sensefly's educational pricing program.